An Information Gain Based Adaptive Path Planning Method for an Autonomous Underwater Vehicle using Sidescan Sonar

Liam Paull, Sajad Saeedi, Howard Li, Vincent Myers

***Abstract*— The majority of path planning research has focused on robots equipped with forward-facing sensors. Algorithms using cell decomposition and information gain are effective at planning paths through obstacle-laden environments, but have not been applied to robots with side-looking sensors whose goal is complete coverage. In addition, the assumptions made about the environment can often prove false, leading to poor mission plans being given by deliberative path planning methods. As a result, adaptive path planning methods which can change the vehicle's path based on *in situ* measurements of the environment are needed.**

In this paper, the information gain approach is extended to apply to adaptive path planning for an autonomous underwater vehicle (AUV) equipped with a sidescan sonar, where the goal is to achieve complete coverage of an area. A new regular exact hexagonal decomposition is used, which is shown to be particularly well suited to side-looking sensors. In addition, the concept of branch entropy in the directed acyclic graph is proposed to help the AUV achieve its global goals while keeping the path planning reactive, a task that is not possible with information gain alone. The results show that for high desired confidence thresholds, the new path planning method with branch entropy outperforms the more conventional information gain approach.

I. Introduction

Sensor path planning refers to the problem of determining a strategy for gathering sensor measurements to support a sensing objective. When the sensors are installed on robotic platforms, an important part of the problem is to plan the path based on sensor readings. Various approaches have been proposed for planning the path of mobile robots with onboard sensors to enable navigation and obstacle avoidance in unstructured dynamic environments. These methods are not directly applicable to robotic sensors whose primary goal is to support a sensing objective, rather than to navigate a dynamic environment in search of a goal. Traditional mission planning methods focus on how the sensor measurements can best support the robot misson, rather than focusing on the robot missions that best support the sensing objective.

Metaheuristic methods using stochastic optimization such as tabu search (TS), genetic algorithms (GA) and simulated annealing (SA) are among the more successful of the motion planning algorithms. In [1], a method based on TS is proposed that performs an iterative visibility scan to find visible obstacle vertices and decides to move toward an obstacle vertex according to a cost criterion. Upon making a move, backward directions are labeled as tabu and excluded from the next set promising directions. If the robot is trapped in a local minimum, it takes a random step toward an unexplored area of the search space and continues its search in the new area. Another method based on GA is proposed in [2] for a holonomic mobile robot. In [3], a combination of SA and the artificial potential field approach is proposed to escape from local minima. In [4], a two layered goal-oriented motion planning strategy is proposed using fuzzy logic. The advantage of this method is that there is no need to have prior knowledge about the environment; however, since the method is a hybrid approach consisting of model and sensor approaches, real-time operation becomes an important issue. An algorithm proposed in [5] based on performing an incremental search on a multi-resolution, dynamically feasible lattice state space has the advantage of real-time performance in high speeds over large distances. The drawback of this method is its sensitivity to dynamic environments which needs collision-free time-parameterized trajectories. In addition, estimating the trajectories of dynamic obstacles accurately is a challenging task due to the uncertainty in these estimates. In [6], greedy based algorithms have been proposed which are based on trapezoidal decomposition of a large field into subfields and selecting the best route among the subfields. The drawback of these methods are their non-optimal results. Another high quality path design avoiding long detours and staying at a safe distance from the obstacles is proposed in [7] and is based on an approximation algorithm used to compute near-optimal paths amidst polygonal obstacles in the plane. This method is optimal but the approximation method can slow down the algorithm in real-time applications. Other traditional model-based path planning techniques are potential fields [8], where essentially the goal attracts the robot and the obstacles repel it, and road mapping [9].

The objective of the present work is to design a path for an autonomous underwater vehicle (AUV) equipped with sidescan sonars (SSS) which acheives complete coverage of an area up to a given confidence threshold. *A priori* knowledge of the environment is not assumed, therefore, the AUV must react and adapt to changes in the environment which affect the sensor performance. As described in Choset's [10] survey of complete coverage methods, there are heuristic, random, and cell decomposition techniques. A heuristic defines a set of rules to follow that will result in the entire environment being covered. For example, Acar and Choset's complete coverage algorithm based on sensing critical points [11], and Wein's [7] method of building corridors based on maximizing some quality function. A key facet of these approaches is having obstacles to be able to generate the rules. Cell decomposition is used to divide up the environment into a managable number of cells or areas that can be searched like a graph or tree. Decomposition can be approximate [12],

semi-approximate, or exact [10]. The shape of the cells and type of decomposition can have a significant impact on the performance of the search algorithm. The exact hexagon cell decomposition method proposed in this paper will be shown to be particularly well-suited to SSS geometry.

Sensor objectives for the coverage task are particularly hard to define because of the uncertainty of sensor measurements. Information gain is exploited as a goodness criterion in the field of machine learning. It measures the number of bits of information obtained for prediction by knowing the presence or absence of certain values and measurements [12]. In this paper, the information gain approach is used in the objective function for the SSS. However, it is shown that the information gain method is not sufficient to achieve global goals when there is incomplete prior information about the environment. To compensate, the concept of branch entropy is proposed. A directed acyclic graph (DAG) is built and the entropy of each branch in the DAG is calculated. The inclusion of this branch entropy term in the measurement benefit function transforms the search from a greedy-first into a reactive A* search.

The novel aspects of this approach include:

- Using information gain (entropy reduction) for SSS, complete coverage, and reactive path planning.
- The exact hexagon cell decomposition which is particularly well-suited to SSS geometry.
- The inclusion of branch entropy in the measurement benefit function.

A detailed description of the problem formulation and assumptions is given in Sec. II. The full methodology is presented in Sec. III. The results are shown in Sec. IV. The conclusions are in Sec. V.

II. Problem Formulation and Assumptions

The task of the AUV is to cover an entire workspace, W, such that the average confidence c_{avg} is greater than some predefined threshold value, c_{thresh} as given by (1), where (i, j) is a point in W.

$$c_{thresh} \leq c_{avg} = \frac{1}{ij} \sum_{i,j \in W} c_{ij}. \tag{1}$$

The AUV enters W with no prior knowledge of the sensor performance. It must make decisions on how to effectively navigate through the environment to achieve the sensing objective using assumptions and information that it gains as it travels in W.

A. Sidescan Sonars

Most path planning research has assumed that the robot is equipped with a forward-looking sensor. In this case, the area covered by the sensor is assumed to be effectively one dimensional; therefore, the sensor only covers an area of the map while the AUV is in motion. In addition, data obtained from the SSS is only considered meaningful while the AUV is in rectilinear motion. Fig. 1 shows an example of the area covered by the sensor, S_A, for a given path, p.

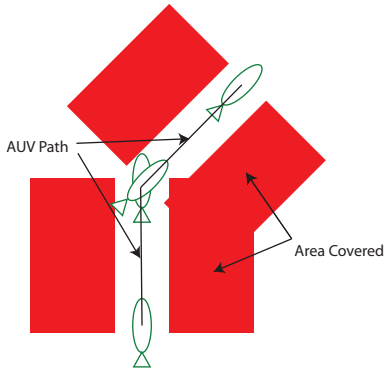

Fig. 1. An example of the AUV path and corresponding area covered by its side-looking sonar.

One of the most important considerations of the SSS framework is that the area directly underneath the AUV is not covered while the AUV is in normal motion. It is assumed that the after n timesteps, the total path p is piecewise rectilinear and can be made as a union of all of the n rectilinear subpaths p_i as given by (2):

$$p = \bigcup_{i=1}^{n} p_i \tag{2}$$

B. Coverage Confidence

It should be noted that the entire area covered by the sensor S_A will not be covered with the same sensor performance. The sensor performance is a function of many factors including the environment, $E = [e_1, e_2, ...e_n]$, where each $e_i, i = 1..n$ represents a different environmental factor such as sea depth or seabed conditions. For a given environment E, the sensor performance is defined by the $\mathcal{P}(y)$ curve which defines the confidence that a target is correctly classified, c , as a function of lateral distance from the AUV, d. Three sample $\mathcal{P}(y)$ curves are shown in Fig. 2, one each for sand, cobble and clay seabed types. The curves are computed using the method described in [13].

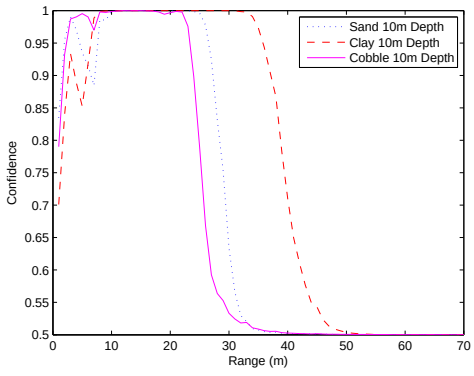

Fig. 2. $\mathcal{P}(y)$ curves for three different seabed conditions

Let T_{ij} represent the existence of a target at each point (i, j), with confidence c_{ij} in W. The probability of detecting

a target, P_{ij} at location (i,j) is given by (3). The confidence value, c_{ij}, therefore, represents the probability that we can accurately predict the existence of a target at location (i,j). The range of P_{ij} is [0,1] but the range of c_{ij} is [0.5,1]. Using (3) and the confidence values read from the $\mathcal{P}(y)$ curve in Fig. 2, the probability P_{ij} of a target existing at point (i,j) can be determined.

$$P_{ij} = \begin{cases} c_{ij} & \text{if } T_{ij} = 1 \\ 1 - c_{ij} & \text{if } T_{ij} = 0 \end{cases} \tag{3}$$

C. Objective Function

In order to plan the path p, each subpath, p_t at time t must be selected to maximize an objective benefit function based on assumptions about the surrounding unknown environment conditions and the data that has been obtained from previous measurements. The objective function is inspired by the one in [12], and is given in (4). B is the information gain, as will be elaborated on in Section III-B, J is proportional to θ, the angle in radians between p_{t-1} and p_t, D is the distance travelled in meters, and G is the branch entropy as will be explained in Section III-D. The weights w_B, w_J, w_D, w_G, represent the weightings for each of the different factors: information gain, turning angle θ, distance travelled, and branch entropy respectively,

$$R(t) = w_B \cdot B(t) - w_J \cdot J(t) - w_D \cdot D(t) + w_G \cdot G(t). \tag{4}$$

At each time t, the membership benefit $R(t)$ is evaluated for each potential path and the one with the most measurement benefit, i.e. highest value of R, is chosen to be followed. The values of B and G contribute positive benefit and should be maximized, whereas the the factors J and B are detremental and should be minimized.

III. Methodology

Previously published methods must be adapted to suit the present problem framework. In this section, algorithms and theory are developed to combine measurements from different incident angles, compute the estimated information gain, obtain the cell decomposition, and compute the branch entropy to be included in the objective function.

A. Combining Measurements

The detection of the targets is conditional upon all of the previous measurements. However, the way that current sensor measurements are combined with previous ones must be known and well defined. In this case, it is assumed that there is a linear relationship between complete dependance and complete independance of two measurements based on the angle, α, between the two measurement incidence angles. Let the two probabilities to be combined be P_1 and P_2 with corresponding angles of measurement θ_1 and θ_2. Without loss of generality, we can assume that $P_1 \geq P_2$ and that $\theta_1 \geq \theta_2$. α is calculated as the acute angle of the intersection of two lines with directions θ_1 and θ_2. Analytically, $\alpha = min(\theta_1 - \theta_2, \theta_1 - \theta_2 - \pi, \theta_1 - \theta_2 - 2\pi)$, such that the range of α is $[0, \pi/2]$.

In the case that the two measurements are parallel, then $\alpha = 0$ and the two probabilities are considered to be dependant: $P_{tot} = P_1$. In the case that the two measurements are perpendicular, then $\alpha = \pi/2$ and the two probabilities are considered to be independant: $P_{tot} = 1 - ((1-P_1)(1-P_2))$. If the angle $0 < \alpha < \pi/2$ then there is a linear relation connecting dependence and independence as described in (5).

$$P_{tot} = \frac{2\alpha P_2}{\pi}(1 - P_1) + P_1 \tag{5}$$

B. Estimated Information Gain

As described in [14], the entropy of a random variable (RV) y given an RV z is:

$$H(y|z) = -\sum_{z^k \in Z} P(y = y^k | z = z^k) \log_2 P(y = y^k | z = z^k). \tag{6}$$

The entropy itself is not as useful as the entropy reduction or information gain. Conditional information gain, I, as defined in (7), is additive and represents the reduction in uncertainty brought about by z_{t+1}, the set of measurements at time $t+1$.

$$I(y; z_{t+1} | z_t) = H(y|z_t) - H(y|z_t, z_{t+1}). \tag{7}$$

In the case when the output is a binary value ($T_{ij} \in \{0, 1\}$) the summation (6) reduces to:

$$H(y|z) = -P\log_2(P) - (1-P)\log_2(1-P), \tag{8}$$

where P represents the conditional probability of detecting a target. The conditional entropy H is symmetrical about the $P = 0.5$, so c can be used directly from the $\mathcal{P}(y)$ curve instead of probability of target detection, P. A high confidence value implies that if there is a target present, it will have a higher chance of being detected.

Given the system state at time t as the set of variables $X_t = [M_t, E_t, T_t]$, then we wish to evaluate the expected information gain that will result from the set of N measurements made by following a particular path p_{t+1}: $M_{t+1} = [M^1_{t+1} M^2_{t+1} ... M^N_{t+1}]$. The expected entropy reduction (EER) then becomes:

$$B(t) = Hy|X_t - \sum_{i=1}^{p} H(y|X_t, M^i_{t+1}). \tag{9}$$

The values of $B(t)$ are caluclated for each of the potential paths to be followed and the values are inserted into the measurement benefit function (4). It should be emphasized that this is only the *expected* entropy reduction. If the environment conditions are unknown, then it is assumed that they are the same as the present location.

C. Exact Hexagonal Cell Decomposition

Cell decomposition is an effective way of reducing the path planning problem into the searching of a tree. Normally, the cells are either exactly or approximately decomposed into rectangloids (i.e. a grid decomposition), although other polygonal shapes have been proposed [6]. However, these decompositions assume that once the AUV moves into a cell, that it is efficiently covered. This assumption is not applicable to the the SSS architecture so a new decomposition method is proposed. The regular hexagon decomposition has the advantage that as the AUV moves from one cell to any adjacent cell, two other cells can be completely covered assuming that the hexagons are sufficiently small. This cell decomposition will result in fewer cells being partially covered.

If W is the workspace to be searched and the cells are C_i for $i = 1..N$ where N is the total number of cells then:

$$\bigcup_{i=1}^{N} C_i = W, \tag{10}$$

and

$$C_i \cap C_j = \emptyset, \forall i = 1..N, j = 1..N, i \neq j, \tag{11}$$

An additional benefit is that the distance, D, can be omitted from the objective function (4) because the distance from the center of any cell to the center of any adjacent cell is the same. Consequently, at each time step the AUV has a maximum of six potential next next locations corresponding to the centers of the six neighbouring hexagons.

D. Branch Entropy

The information gain method has been shown to be effective for solving the path planning problem when *a priori* knowldege of the environment, obstacles, and targets is available. However, it is common that this information will not be available, or will not be completely accurate. As a result, the AUV must be able to be reactive. In the reactive approach, the information gain B is useful for evaluating the benefits of each of the potential next moves, but when complete coverage is the goal, this approach reduces to a greedy-first search (GFS).

It is necessary to include a parameter in the objective function that helps the AUV to achieve its global goal. This parameter is coined the branch entropy (BE) and transforms the GFS into a reactive A* search. The benefits of including the BE in the objective function are:

- It helps the AUV finish sections before it leaves them.
- It allows the AUV to find the areas of the graph that are left undone.
- It acts as a tiebreaker so that the AUV never enters infinite loops.

1) Building the Directed Acyclic Graph: The Directed Acyclic Graph (DAG) is built such that every cell C_i appears only once in the graph, and is at level l, where l is the miniumum number of steps that could be taken to get from the present cell C_p to C_i. There can be several paths from C_p to C_i but they must all be the same minimum length. The value v_i of each node in the graph is the average entropy of the cell C_i. A major advantage of the hexagon decomposition is that each cell at level l is the same path distance from C_p.

Each neighbour of C_p becomes a child in the graph. The neighbours of those nodes become children provided they are not already in the graph at higher level. This process continues until all cells are in the DAG.

The DAG is built using the following pseudocode where C_p is the current cell and C is the set of all cells:

procedure $build\_graph(C, C_p)$
  $DoneList \leftarrow C_p$
  $level \leftarrow 1$
  while $DoneList \neq C$ **do**
    $level \leftarrow level + 1$
    for $n \leftarrow$ Each node in $level - 1$ **do**
      $CurrentList \leftarrow \emptyset$
      $n.children \leftarrow \emptyset$
      for $k \leftarrow$ All neighbors of n **do**
        if $k \notin DoneList$ **then**
          $n.children \leftarrow n.children \cup k$
          $k.value \leftarrow C_k.entropy$
          if $k \notin CurrentList$ **then**
            $CurrentList \leftarrow CurrentList \cup k$
          end if
        end if
      end for
    end for
    $DoneList \leftarrow DoneList \cup CurrentList$
  end while

2) Derivation of Branch Entropy: The BE is used to evaluate how much entropy there is down each branch of the DAG. Some preference will be given to the move that takes the AUV towards an unfinished area of W. Also, priority will be given to moves that have more unfinished area nearer to the current position so that the AUV does not leave an area before it is finished.

There will be a value of BE for each neighbour of the current cell C_p as each neighbour has its own branch in the DAG. In order for the BE to provide the benefits desired, cells that are at higher levels in the graph must be given more weight. For each neighbor, $k = 1..K$, of C_p, the BE, G, for a DAG with a total of L levels is given by (12). m_l is the number of nodes in level l of branch k and H_i is the average entropy of cell C_i.

$$G_k = \frac{\sum_{l=2}^{L}(L-l+1)\frac{\sum_{i=1}^{m_{lk}} H_i}{m_{lk}}}{\sum_{l=1}^{L-1} l}. \quad (12)$$

3) Simple Example: Fig. 3 shows the transformation from hexagon cells to DAG. The cell labeled C_p is the cell that the AUV is currently in, and the values in all of the other cells represent their average entropies.

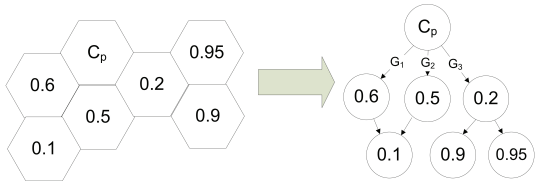

Fig. 3. A transformation from Cell to DAG. (numbers in cells/nodes represent average cell entropy)

The corresponding BE for each of the three neigbours are calculated as:

$$\begin{aligned} G_1 &= 1/3((2)(0.6)+(1)(0.1)) = 0.433, \\ G_2 &= 1/3((2)(0.5)+(1)(0.1)) = 0.367, \\ G_3 &= 1/3((2)(0.2)+(1)(1/2)(0.95+0.90)) = 0.442. \end{aligned} \quad (13)$$

From the calculations, the third branch would get the highest G value but the choice of which cell to move to next depends on the evaluation of the measurement objective function (4).

IV. Results

The workspace W is a 100 meter square. W is divided into four quadrants and each is either cobble , sand, or clay. The $\mathcal{P}(y)$ curves are given in Fig. 2. The step-size is chosen as 10m.

A. Information Gain

Fig. 4 shows the path obtained for $c_{thresh} = .99$ using the information gain approach. Some targets were randomly added to the map and simulated.

B. Information Gain with Branch Entropy

Fig. 5 shows the path obtained for $c_{thresh} = .99$ with the branch entropy term included in the objective function.

In Fig. 6, the final achieved confidence over the entire workspace is shown. The colours at the bottom correspond to different environmental conditions: blue is cobble, red is clay, and yellow is sand.

Table. I shows the results of the simulation for random search, information gain approach, branch entropy, each for three different confidence thresholds. It is important to note

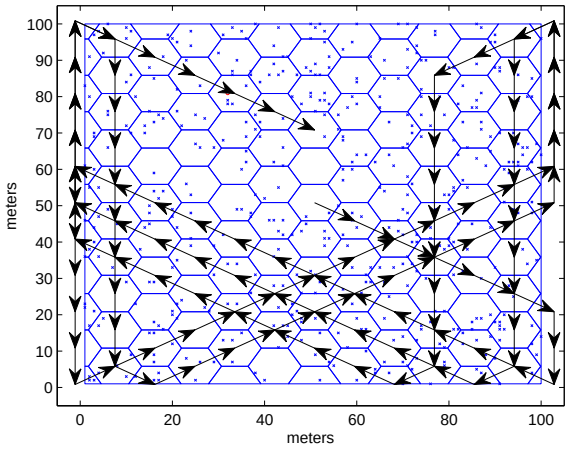

Fig. 4. path and targets detected (blue x's) and not detected (red o's) using information gain alone with confidence threshold = .99

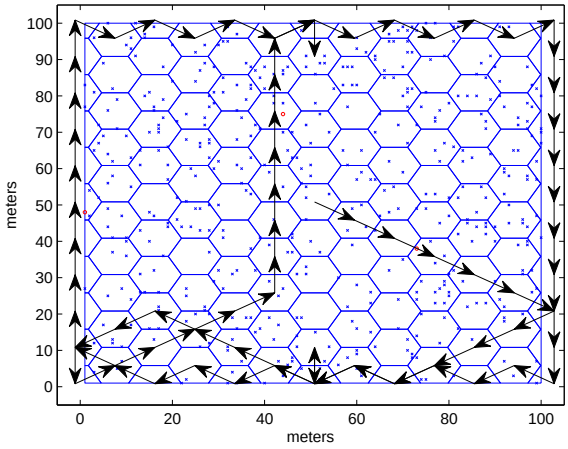

Fig. 5. Path and targets detected (blue x's) and not detected (red o's) using branch entropy with confidence threshold = .99

that the detection rate is not guaranteed to be higher than c_{thresh}, however the mean of the detection rate over repeated trials is guaranteed to be higher than c_{thresh}.

From the results, the branch entropy method outperforms the information gain alone, particularly in the case where the confidence threshold is very high. For the case where c_{thresh} was 99%, the information gain method required 1270m of distance travelled and 62.0 total radians turned, but branch entropy method travelled only 790m and turned 49.7 rads to cover the entire workspace.

V. Conclusion

A framework is developed for the reactive path planning of a Autonomous Underwater Vehicle (AUV) equipped with a sidescan sonar (SSS). The AUV uses information gain, distance travelled, angle turned, and branch entropy to make decisions. The information gain is defined as the expected entropy reduction over the entire map that would result if that move was made.

Search Algorithm	c_{thresh}	Path Length (m)	Total Angle Turned (rads)	Detected Targetss	Undetected Targets	Detection Rate (%)
Random Search	.90	1820	306	454	41	91.7
Random Search	.95	2940	475	485	21	95.9
Random Search	.99	6660	1051	498	6	98.9
Information Gain	.90	460	30.0	468	33	93.4
Information Gain	.95	520	37.2	486	24	95.3
Information Gain	.99	1270	62.0	479	1	99.8
Branch Entropy	.90	390	25.5	486	37	92.9
Branch Entropy	.95	500	30.1	524	18	96.7
Branch Entropy	.99	790	49.7	484	3	99.4

TABLE I

PERFORMANCE OF RANDOM SEARCH, INFORMATION GAIN AND INFORMATION GAIN WITH BRANCH ENTROPY ALGORITHMS FOR DIFFERENT CONFIDENCE THRESHOLDS

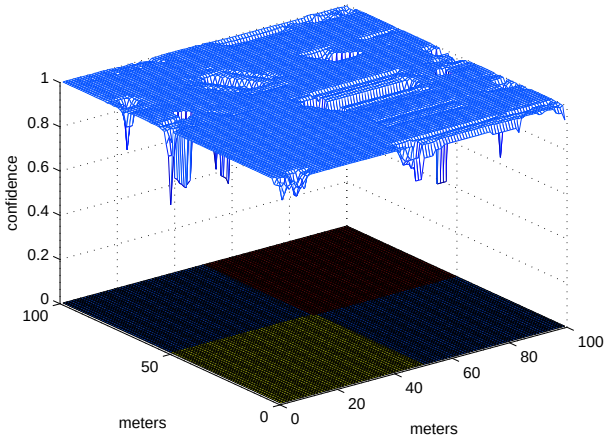

Fig. 6. Achieved confidence over workspace. Colours on confidence = 0 axis correspond to subsections of workspace with different environmental conditions.

The branch entropy is used to help the AUV achieve its global goals. A directed acyclic graph is built using an exact hexagon decomposition over the entire search area, and then the branch entropy is defined according to (12). The inclusion of the branch entropy in the objection function has many benefits: it helps the AUV finish areas before it leaves, it allows the AUV to find areas of workspace that are unsearched, and it resolve ties to prevent infinite loops. The results show that branch entropy method outperforms information gain alone, particularly when the desired confidence level is very high.

REFERENCES

[1] Ellips Masehian and Mohammad Reza Amin-Naserin, "Sensor-based robot motion planning," *IEEE Robotics and Automation Magazine*, vol. 15, no. 2, pp. 48–57, June 2008.

[2] Talbil El-Ghazali Juan Manuel Ahuactzin, Pierre Bessiere and Emmanuel Mazer, "Geometric reasoning for perception and action," *Springer Berlin/Heidelberg*, vol. 708, pp. 83–84, 1993.

[3] F. Janabi-Sharifi and D. Vinke, "Integration of the artificial potential field approach with simulated annealing for robot path planning," *Proc. IEEE Int. Symp. Intell. Contr*, pp. 536–541, August 1993.

[4] Mehrdad Moallem Xiaoyu Yang and Rajni V. Patel, "A layered goaloriented fuzzy motion planning strategy for mobile robot navigation," *IEEE Transactions on Systems, Man, and Cybernetics. Part B: Cybernetics*, vol. 35, no. 6, pp. 1214–1224, December 2005.

[5] Maxim Likhachev and Dave Ferguson, "Planning long dynamically feasible maneuvers for autonomous vehicles," *The International Journal of Robotics Research*, vol. 28, no. 8, pp. 933–945, August 2009.

[6] Timo Oksanen and Arto Visala, "Coverage path planning algorithms for agricultural field machines," *Journal of Field Robotics*, vol. 26, no. 8, pp. 651–668, August 2009.

[7] Jur VanDenBerg Ron Wein and Dan Halperin, "Planning highquality paths and corridors amidst obstacles," *The International Journal of Robotics Research*, vol. 27, no. 11-12, pp. 1213–1231, November/December 2008.

[8] Yong K. Hwang and Narendra Ahuja, "A potential field approach to path planning," *IEEE Transactions on Robotics and Automation*, vol. 8, no. 4, pp. 23–32, 1992.

[9] P. Bhattacharya and M.L. Gavrilova, "Roadmap-based path planning using the voronoi diagram for a clearance-based shortest path," *IEEE Robotics and Automation Magazine*, vol. 15, no. 2, pp. 58–66, June 2008.

[10] Howie Choset, "Coverage for robotics - a survery of recent results," *Annals of Mathematics and Artificial Intelligence*, vol. 31, pp. 113–126, 2001.

[11] Ercan U. Acar and Howie Choset, "Sensor-based coverage of unknown environments: Incremental construction of morse decompositions," *International Journal of Robotics Research*, vol. 21, pp. 345–367, 2002.

[12] Cheghui Cai and Silvia Ferrari, "Information-driven sensor path planning by approximate cell decomposition," *IEEE Transactions on Systems, Man, and Cybernetics - Part B: Cybernetics*, vol. 39, no. 3, pp. 672–689, June 2009.

[13] Vincent Myers and Marc Pinto, "bounding the performance of sides-can sonar automatic target recognition algorithms using information theory," *IET Radar Sonar and Navigation*, pp. 226–273, 2007.

[14] Athanasios Papoulis and S. Unnikrishna Pillai, *Probability, Random Variables and Stochastic Processes*, McGraw Hill, fourth edition, 2002.